Crystals and inclined conduits:
analogue experiments for slug-driven volcanism

🆔 Hannah Calleja*[α] and 🆔 Tom D. Pering[β]

[α] University of Edinburgh School of GeoSciences, Kings Buildings, W Mains Rd, Edinburgh EH9 3JW, UK.
[β] University of Sheffield Department of Geography, Winter St, Sheffield S3 7ND, UK.

ABSTRACT

Basaltic volcanism is the dominant mode of volcanism on Earth and exhibits a range of activity, from passive degassing to the most common explosive style: Strombolian volcanism. Strombolian volcanism is driven by gas slugs, making it vital to consider the effects of variable magma rheology and internal vent geometry on slug flow dynamics. Experimental technologies play a major role in developing our understanding of the natural complexity of such basaltic systems. This study examines slug ascent within particle-free and particle-bearing media experimentally across a range of inclinations. Dimensionless parameters are derived to describe specific flow characteristics at laboratory and volcanic scales, and to demonstrate the viability of current theoretical framework. Slug ascent is shown to be dependent on its morphology, which is a function of inclination, liquid viscosity, and related controlling characteristics i.e. particle fraction. Maxima for ascent velocities and associated dimensionless parameters occur within the range 40–60°.

NOMENCLATURE

v_b	slug ascent velocity, $\mathrm{m\,s^{-1}}$
d	distance, m
t	time, s
N_f	inverse viscosity
L_b	slug length, cm
D_b	slug diameter, cm
θ	tube inclination angle, °
Fr	Froude number
Re	Reynold number
μ	viscocity, $\mathrm{Pa\,s}$
ρ	density, $\mathrm{kg\,m^{-3}}$
D	tube/conduit diameter, m
g	gravitational acceleration, $\mathrm{m\,s^{-2}}$
PVF	particle volume fraction, refers to experimental contexts
CVF	crystal volume fraction, refers to true scale

1 INTRODUCTION

Knowledge of volcanic eruption styles and forecasting relies on our understanding of the physics of coupled (one-phase) or uncoupled (multi-phase) magma–gas behaviour in shallow plumbing systems [Parfitt 2004]. Basaltic systems commonly exhibit open-vent characteristics where gas can ascend freely and burst at the free magma surface [Mintz et al. 2021]. Bubble formation is triggered by the sudden exsolution of a limited gas volume into the surrounding magma [Sparks 1978; 2003]. Bubbles are initially small until they expand, collide, and coalesce during ascent and can—given a high enough gas supply—eventually generate large classes of bubbles called slugs, driven by the decreasing solubility of H_2O in silicate melts as pressure decreases towards the surface [Sparks 1978; 2003; Edmonds et al. 2014]. Basaltic systems can exhibit a variety of eruption styles with variable intensity within short time periods [Houghton et al. 2016; Gaudin et al. 2017; Jones et al. 2022] but slug flow dynamics are predominantly discussed as drivers of Strombolian activity.

Slugs (Figure 1) are conduit-filling bubbles whose length are greater than 1.5 times their diameter [Shosho and Ryan 2001; Llewellin et al. 2012]. They are well studied and reported in the literature because they generate a range of explosive eruptions, from variable Strombolian activity [Houghton et al. 2016] to violent paroxysms [Viccaro et al. 2021]. Ergo, our current understanding of in-conduit flow dynamics can largely be attributed to their study in recent decades. Slug volume, and thus their internal pressure, heavily influences slug overpressure and thus explosivity at burst [Vergniolle and Jaupart 1990; James et al. 2008; Del Bello et al. 2012]. This occurs when the internal pressure exceeds the external pressure in the surrounding magma during ascent and triggers the acceleration of the overlying liquid [Moitra and Gonnermann 2015; Oppenheimer et al. 2020]. The characteristics of slug ascent are largely described to be a function of source depth (i.e. the point that gas stops re-equilibrating) and inter-bubble interaction [Jaupart and Vergniolle 1989; Seyfried and Freundt 2000; James et al. 2008; Pering and McGonigle 2018], vent geometry [James et al. 2004; 2006; Spina et al. 2019], and magma rheology [Del Bello et al. 2015; Oppenheimer et al. 2015; Barth et al. 2019; Woitischek et al. 2020] in existing literature.

Magma is a mixture of silicate melt containing crystals and dissolved volatiles [Oppenheimer et al. 2015]; flow behaviour is determined by the ratio of these attributes within the magma, as well as melt pressure and temperature. Specific crystal fraction affects relative viscosity—the ratio of melt phase to mixture viscosity—over several orders of magnitude [Caricchi
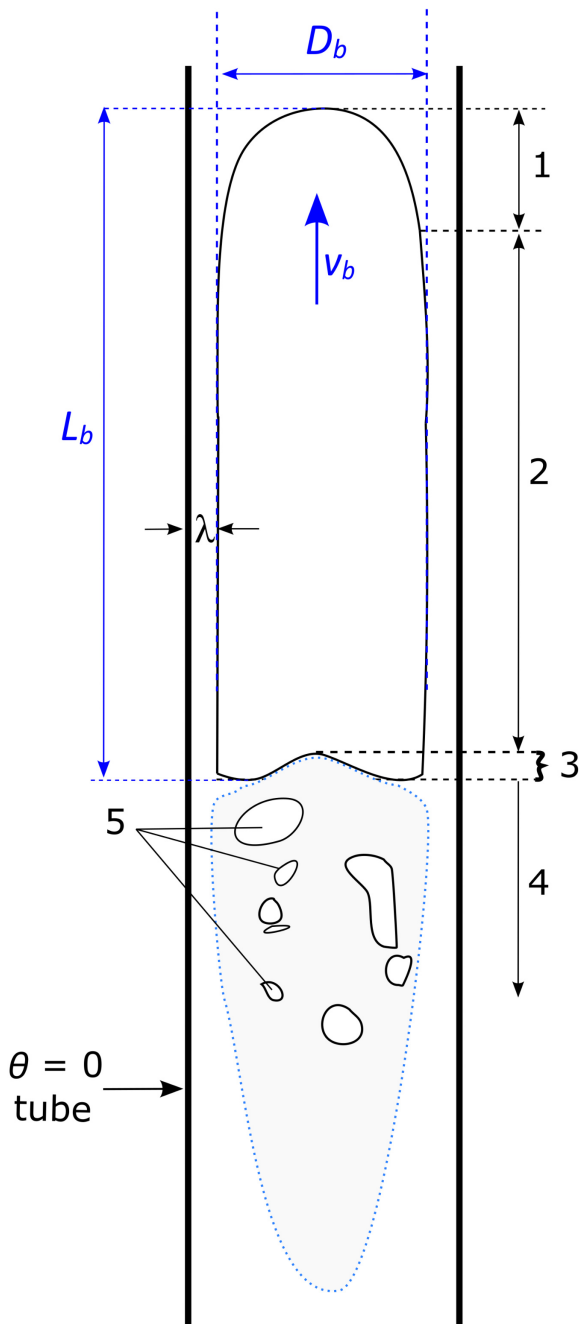
Figure 1: Schematic showing typical slug structure under laminar flow in a vertical cylindrical conduit. Structural parameters are shown in black: 1 – nose, 2 – body, 3 – tail, 4 – wake and wake interaction length as indicated by 5 – recirculating trailing bubbles, λ – liquid falling film. The parameters we measure are indicated by blue font: L_b – slug length, D_b – slug diameter, v_b – ascent velocity. Slug shape is also traced for morphological observations.

et al. 2007; Moitra and Gonnermann 2015] and an increase in crystal fraction is generally thought to increase relative viscosity as flow slows down to deviate around them [Parfitt 2004;

Moitra and Gonnermann 2015]. For clarity and from this point on, crystal volume fraction (CVF) and particle volume fraction (PVF) will be used to refer to the amounts of crystals, and crystal analogue material within volcanic and experimental contexts, respectively. Particle shape is shown to have notable influence on fluid viscosity in experimental contexts, but a robust relation between magmatic viscosity and specific crystal morphology in volcanic contexts is lacking. Most simple slug burst models are based on rheologically uniform media [e.g. James et al. 2008; Del Bello et al. 2012]. Barth et al. [2019] highlighted the role that particle rich layers could have in generating slugs, while Oppenheimer et al. [2015] noted that the generation of larger slugs was inhibited when PVF rose above 55 %. The presence of a rheologically thicker cap has been hypothesised at Stromboli [Del Bello et al. 2015; Capponi et al. 2016], while Oppenheimer et al. [2020] note that larger slugs can be disrupted at particle volume fractions as low as 30 %. Eruption style is dependent on both gas and magma availability, so characterising the effects of crystals on both magma rheology and slug flow dynamics is vital to the estimation of subsurface and surface activity.

Uniform cylindrical tubes are by no means perfect analogues for the real internal geometry of volcanic conduits: kinks, flares, internal diameter variations, conduit roughness, storage zones, and internal obstacles are all common features in active shallow plumbing systems. This study focuses on conduit inclination, for which there is evidence at several active locations worldwide. At Stromboli (Italy), seismic waveform inversion suggests a conduit with a 40° dip angle [Chouet et al. 2003]. Similarly, Yamamoto et al. [1999] discovered an inclined crack-like conduit at Aso (Japan) using long period tremor. Several lines of evidence including a lack of direct imaging of the uppermost conduit, moment tensor, and tomographic results indicate an average terminal conduit dip of ~60° at Erebus, Antarctica [Zandomeneghi et al. 2013; Knox et al. 2018]. Meanwhile, at Masaya, Pering et al. [2019] hypothesised that an inclined conduit explained the variation in bubble burst behaviour at the free magma surface of the lake. Each magmatic and geometric complexity has its own individual variability and thus impact on slug ascent behaviour and surface explosivity, making the modelling of these processes extremely complicated. It is for this reason that these complexities are so rarely accounted for in experimental literature. Here, we consider the combined effects of crystals at low particle fractions (<10 %) and conduit inclination (0–70°) on slug flow parameters using a suite of experiments.

2 THEORETICAL FRAMEWORK AND EXPERIMENTS IN THE LITERATURE

Details surrounding slug flow are comprehensive in volcanic literature because of their relation to explosive eruption styles in low viscosity magmas. Slugs have also been described extensively in the engineering literature [see the review of Morgado et al. 2016]. Slug formation, structure, and behaviour has been a major research focus in past decades [Davies and Taylor 1950; Seyfried and Freundt 2000; James et al. 2009; Kawaguchi and Nishimura 2015; Pering and McGonigle 2018, and those listed below]. The theoretical framework for slug

ascent within rheologically uniform liquids in vertical conduits is robust due to their wide range of applications in industry, where they are commonly referred to as Taylor bubbles [Davies and Taylor 1950; Bugg and Saad 2002; Viana et al. 2003; de Azevedo et al. 2012]. Numerous experimental studies of two-phase slug flow that focus on ascent velocity [White and Beardmore 1962; Zukoski 1966; Campos and Guedes De Carvalho 1988; Seyfried and Freundt 2000; Shosho and Ryan 2001], morphology [Seyfried and Freundt 2000; de Azevedo et al. 2012], coalescence [Pinto et al. 1998; Pering et al. 2017], the liquid flow patterns that surround slugs [Kawaji et al. 1997; Bugg and Saad 2002; Llewellin et al. 2012], and acoustic measures of overpressure [James et al. 2004; 2006; 2008; Spina et al. 2019] have been performed across both disciplines.

Quantitative experimental studies for slug ascent outside of these conditions are scarce, especially within the context of volcanism. James et al. [2004] is one of the only volcanic studies that investigates the effect of tube inclination on slug dynamics and relates findings to true-scale gas-dynamics. Several papers investigate slug ascent velocity as a function of pipe inclination in engineering contexts [Zukoski 1966; Bendiksen 1984; Nigam et al. 1995; Shosho and Ryan 2001; Pokusaev et al. 2011; de Azevedo et al. 2015; Rana et al. 2016; Massoud et al. 2020], which provide a starting point for our own investigation of this parameter. Recent work introduces the concepts of crystal packing [Woitischek et al. 2020], stratified magma rheology [Del Bello et al. 2012; Capponi et al. 2016; Barth et al. 2019], or a combination of both [Oppenheimer et al. 2020] to slug experiment setups. However, current models cannot suitably explain the natural system complexity exposed by geochemical and petrological analyses of ejecta [Capponi et al. 2016]; most analogue-based theoretical models for basaltic volcanism neglect the presence of crystals altogether and only consider slug flow in rheologically uniform media [James et al. 2004; 2006; 2008; Suckale et al. 2010a; Suckale et al. 2010b; Pering et al. 2016; Pering and McGonigle 2018].

Existing theoretical framework is centred solely on slugs rising in an assumed cylindrical and vertical conduit within Newtonian media. Under these (experimental) conditions slug ascent velocity, v_b, is a known function of fluid viscosity, μ, density, ρ, surface tension, σ, internal tube diameter, D, and gravitational acceleration, g, [Seyfried and Freundt 2000; James et al. 2004; 2008; Llewellin et al. 2012; Del Bello et al. 2015; Capponi et al. 2017]. Measured bubble parameters can then be combined with liquid and conduit properties to calculate dimensionless numbers, which provide a numerical description of fluid flow that is applicable to both laboratory and volcanic scales, as derived from the following equations [Wallis 1969; Seyfried and Freundt 2000; Shosho and Ryan 2001; Llewellin et al. 2012]. The dimensionless inverse viscosity, N_f:

$$N_f = \frac{\rho\sqrt{gD^3}}{\mu} \qquad (1)$$

the bubble Reynolds number, Re:

$$Re = \frac{\rho v_b D}{\mu} \qquad (2)$$

and the Froude number, Fr:

$$Fr = \frac{v_b}{\sqrt{gD}}. \qquad (3)$$

N_f is defined as the ratio of external to internal forces. It is also used to categorise flow patterns in slug wakes. Re describes the ratio of inertial to viscous forces within a flow and is often used as an indicator of turbulence in both experimental and volcanic contexts because of its implications for slug formation and stability. Fr is a dimensionless velocity parameter used to describe the influence of gravity (or buoyancy) on fluid motion, i.e. the flow pattern over an obstacle such as the liquid film flowing around a bubble or the deviation of flow around particles, if any are present.

Fr and Re are particularly important in the context of this study because they are a direct function of v_b, and thus provide some vital, though currently rudimentary insight into internal magma–gas pathway dynamics. A simple derivation of the Fr equation is used to estimate the ascent velocity of volcanic slugs in the current literature:

$$v_b = Fr\sqrt{gD} \qquad (4)$$

originally demonstrated by Wallis [1969] and later literature, or

$$U_{sl} = \sqrt{2gr_c} \qquad (5)$$

as displayed in Pering et al. [2017], where U_{sl} represents the (assumed constant) base velocity of a rising slug within a volcanic conduit, and r_c is conduit radius. As demonstrated in Equation 3, Fr cannot be calculated without first quantifying slug ascent velocity, which cannot be directly observed inside a volcanic conduit (although passage can be implied through geophysical means [Chouet et al. 2003]). Viana et al. [2003] solved for ascent velocity by observing that in vertical conduits, Fr is a function of N_f and Eo, independently of v_b when interfacial tension effects are negligible (when $Eo > 40$, a boundary commonly exceeded in volcanic settings) and flow is laminar (when $Re < 2000$). They introduced a universal empirical correlation for Fr under these conditions, which was simplified by Llewellin et al. [2012] to give:

$$Fr = 0.34\left[1 + \left(\frac{31.08}{N_f}\right)^{1.45}\right]^{-0.71} \qquad (6)$$

where Fr is derived as a function of N_f only. While this covers a very broad validity range of $10^{-1} < N_f < 10^5$, it is restricted to the parameters explored within their specific experimental system and thus lacks the complexity of true scale flow behaviour. Re can also be written as a function of N_f and Fr (Equation 7) only as an alternative for calculating true scale estimates, but also relies on the Fr correlation and thus offers the same limitations:

$$Re = N_f Fr. \qquad (7)$$

Current equations that estimate volcano-scale flow behaviour are based on slug flow experiments in rheologically
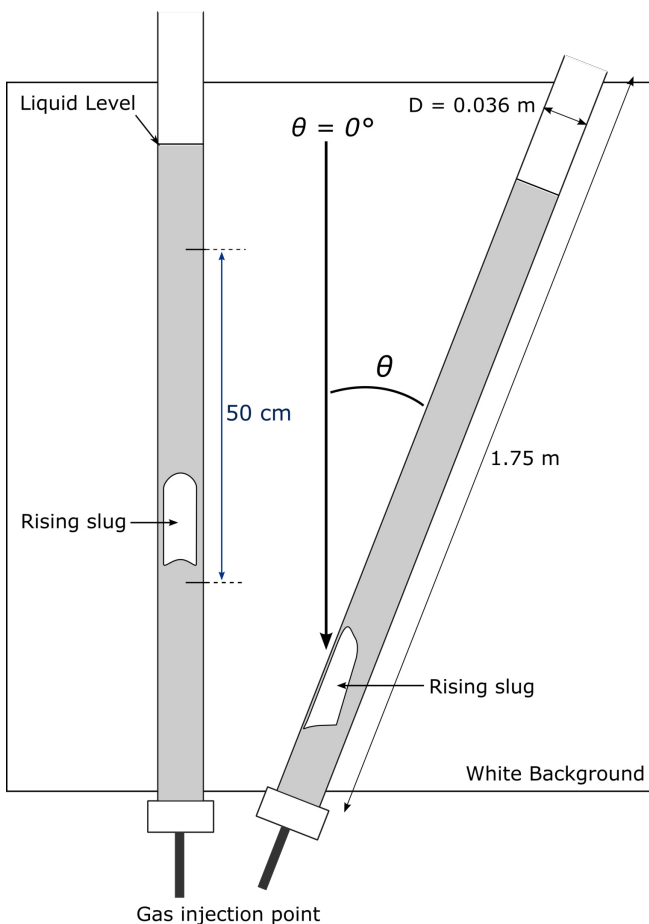
Figure 2: Experiment setup. Transparent acrylic tubing with internal diameter, D = 0.036 m, filled with glycerol solutions (particle-containing and particle-free; 0.09–0.343 Pa s) to 90 % capacity to prevent spillage. Measurements cover a range of inclinations (0–70°). An airline control valve and gas syringe was used for isolated 50 mL slug injections recorded with a Canon EOS 5D Mark IV DSLR camera (standard wide-angle lens) at 120 fps, located 2 m from the tube in bright, natural lighting. Temperature probes were used to indicate the impact of temperature fluctuations on liquid viscosity (negligible; maximum fluctuation from ambient: ±5 °C).

Table 1: A summary of liquid properties.

	Glycerol content wt.%	μ Pa s	ρ kg m^{-3}	N_f	PVF* %
PVF 0	60	0.004	1188	6354	–
	70	0.042	1216	619	–
	80	0.077	1244	345	–
	90	0.171	1258	158	–
	100	0.82	1298	34	–
PVF 1	60	0.005	1169	4561	2.6
	70	0.053	1133	459	2.2
	80	0.079	1128	306	1.8
	90	0.193	1189	132	2.2
	100	1.043	1208	25	2.7
PVF 2	60	0.05	1176	500	3.5
	70	0.065	1191	393	3.6
	80	0.093	1219	280	3.8
	90	0.332	1245	80	5.1
	100	1.512	1267	18	6.1

* True PVF was calculated by subtracting empty volume from maximum expected fill volume.
PVF 0, 1, and 2 refer to particle-free and PVF mixtures with lowest and highest average particle content, respectively.

uniform media and cylindrical vertical tubes only as a direct result of the *Fr* empirical correlation and its assumptions. While the literature demonstrates an awareness of complex flow conditions within real volcanic plumbing systems [Seyfried and Freundt 2000; James et al. 2004; Pering et al. 2017; Spina et al. 2019; Oppenheimer et al. 2020; Silva et al. 2023] the theoretical consideration of these is sparse. It is therefore vital to expand our existing theoretical frameworks to accommodate for complex magma rheology and conduit geometries in order to increase our understanding of magma–gas flow dynamics. One way of achieving this is through analogue experimentation.

3   METHODS

The setup (Figure 2) is low-cost, versatile, and based on previous studies in volcanic and engineering literature and our own preliminary work [Calleja and Pering 2021]; we adapt our experiments to accommodate the addition of inclination and a crystal analogue. Slug ascent is recorded in open ended vertical and inclined tubing containing a range of media properties (with and without particles; Table 1) that can be suitably scaled up for comparison with real volcanic scenarios. This study explores the implications of complexities on single slug ascent only, so the implications of bubble expansion, inter-bubble interaction, other gas regimes (spherical, spherical cap, etc.), and conduit geometries other than inclination are neglected. The setup cannot effectively capture the full range of disequilibrium observed in real volcanic systems but it represents a necessary oversimplification of real subsurface complexities that allows for control over experimental parameters in a way that is theoretically manageable.

We generated selection criteria for an appropriate crystal analogue with suitable properties for both experimental and volcanic scaling applications (Table 2). Strombolian volcanism is the endmember eruption style for gas-crystal interaction in basaltic magmas (CVF = 30–55 vol.%) and represents the ideal CVF range for slug-driven behaviour at true scale [Caricchi et al. 2007; Giordano et al. 2010; Oppenheimer et al. 2020]. It is succeeded by lava fountaining and corresponding annular flow from high gas content and low magmatic viscosity [CVF ~ 35 vol.%; Giordano et al. 2010; Oppenheimer et al. 2015]. The true PVF range for this study is 1.8–6.1 vol.%; this is a lower range relative to existing studies due to experimental constraints associated with slug visibility that occur above our maximum PVF. Individual mixtures have separate PVF values

Table 2: Particle selection criteria for an appropriate crystal analogue.

Criteria Type	Criteria
Particle Size	Crystal to conduit diameter ratio; e.g. 0.001:3 m for Stromboli; 0.005:4 m for Yasur [Woitischek et al. 2020] which scale down comparably to $D = 0.036$ m tube used here, i.e. ~10–50 µm analogue particles would be ideal.
Particle Shape	Organic, asymmetric particles are more appropriate due to non-uniformity of real magmatic crystals. Several studies use uniformly shaped glass or plastic beads [Vona et al. 2011; Oppenheimer et al. 2015; Oppenheimer et al. 2020; Woitischek et al. 2020].
Density, ρ	Determines the rate at which analogue particles settle into surrounding liquid; if $\rho \leq$ surrounding liquid, particles float or remain in suspension (ideal experimental scenario). If $\rho >$ surrounding liquid, particles settle out and cause blockages.
PVF and CVF	Caricchi et al. [2007] classified particle fraction by weight: 50–80 wt.%, they classify <30 % as low crystal content and >30 % as 'crystal rich' mixtures. Oppenheimer et al. [2020]: Strombolian activity ejecta CVF >30 %; rise dynamics somewhat affected at CVF ≤ 30 vol.% but bubble deformation is clearest when CVF > 38 vol.%. High crystallinity: 20–40 vol.% CVF. Giordano et al. [2010]: CVF > 55 vol.% (endmember for Strombolian activity) and CVF ~ 35 vol.% (Hawaiian) from textural analysis of eruptive products from Etna.
Chemical Properties	Dissolution problem (experimental): depending on material, particles may dissolve into surrounding solution, thus affecting actual PVF. Increased dissolution also inhibits visibility. Non-organic materials, e.g. plastic microbeads, are chemically inert but expensive and have adverse environmental impacts, thus were avoided.
Accessibility and Safety	Low-cost, readily available in large quantities (material lost during sieving), with no risk of adverse reaction (ideally edible) or respiratory concern [especially small particles <75 µm; World Health Organization 2002].

Materials tested	Material suitability
Crushed sand	Too dense and large, settled immediately.
Crushed quartz	Too dense and large, settled immediately.
Acid-washed kaolin	Slugs not visible.
Silts	Caused blockages at injection point and valves
Pepper	Hydrophobic, i.e. floats.
Cinnamon powder	Chosen analogue: Some visibility issues (mostly resolved during footage processing). Stayed in suspension ($\rho = 446$ kg m^{-3}), appropriate shape and size, safe, easy to source cheaply in large quantities.

Table 3: The structural parameters of slugs measured across 0°, 40°, and 70° inclinations.

| | | L_b (cm) | | | | | D_b (cm) | | | | |
| | | Glycerol solution (wt.%) | | | | | Glycerol solution (wt.%) | | | | |
	θ	60	70	80	90	100	60	70	80	90	100
PVF 0	0	6.54	7	7.66	7.86	9.14	3.51	3.62	3.56	3.61	3.25
	40	8.49	8.34	9.1	9	9.55	2.6	2.26	2.41	2.42	2.35
	70	10.29	10.6	11.34	10.83	13.47	2.3	2.17	2.19	2.25	1.84
PVF 1	0	6.56	6.11	6.69	7.22	8.48	3.65	3.58	3.48	3.47	3.96
	40	9.36	8.81	8.9	8.57	9.75	2.38	2.23	2.22	2.08	1.75
	70	11.41	11.69	11.45	10.86	14.14	2.12	2.1	2.06	1.86	1.57
PVF 2	0	–	–	–	–	–	–	–	–	–	–
	40	10.09	8.96	9.59	8.08	–	2.22	2.18	2.3	2.06	–
	70	11.28	11.57	10.77	10.42	15.24	1.99	2.13	2.11	1.79	1.91

Dashes indicate gaps in the dataset due to visibility issues.

(Table 1) so we categorize mixtures as PVF 0, PVF 1, and PVF 2 for clarity, i.e. particle-free and average least to most particle-bearing mixtures, respectively.

Particle size (Figure 3) can be scaled to the ideal crystal to conduit ratio based on known values in natural systems. For example, shallow magma from Stromboli where slug-driven Strombolian eruptions occur produce maximum crystal dimensions of ~5 mm (5000 μm) for clinopyroxene, 3–4 mm (3000–4000 μm) for olivine, and ~2 mm (2000 μm) for plagioclase [Armienti et al. 2007]. If we take a typical conduit diameter of ~3 m [Chouet et al. 2003] we can estimate a crystal to conduit ratio of ~0.0007–0.002. Applying this to our tube diameter yields an appropriate crystal analogue dimension of ~25–72 μm. However, the particles utilised in our experiments are not perfectly scaled to the ideal crystal to conduit ratio estimate for respiratory safety and because sieving yielded very little material of this size. Despite this, actual particle size (125–500 μm) used here aligns similarly with particle size ranges used in studies that closely resemble our experiments. Oppenheimer et al. [2020] used 800 μm polypropylene particles (irregularly shaped) in tubes of diameter 0.0257 m, giving a crystal to conduit ratio of 0.03. Meanwhile, Woitischek et al. [2020] used 2 μm particles in a 0.02 m conduit, giving a crystal to conduit ratio of 0.0001. Our particle analogue (125–500 μm and a ratio of ~0.003–0.01) falls within the range for crystal dimensions at Stromboli or for those with larger crystal populations such as Yasur, Vanuatu [Métrich et al. 2011].

Liquid media (60–100 wt.% glycerol) are made by mixing 100 wt.% glycerol with deionised water by weight (e.g. 400 g deionised water to 600 g glycerol for a 60 wt.% solution). The appropriate amounts of crystal analogue are determined by volume (e.g. particles packed into a $D = 0.036$ m tube offcut to fill 6 vol.% of the total tube fill volume for PVF 2) then added to each solution and left to settle; they are stirred before use. This method, the action of gas injection, and the anticoagulant properties of glycerol minimise particle clumping. Relevant mixtures are made up just before the recording of relevant runs to reduce particle settling once in the tube. The action of gas injection further inhibits particle settling and maintains an even particle distribution throughout the tube during measurement. All footage is organised then converted into an appropriate file format (.avi with conserved metadata) for bubble analysis in imageJ*. Individual videos (i.e. individual experiment runs) are broken down into frames, then pixel distance is converted to the appropriate unit using a known distance such as internal tube diameter. Morphology measurements for each recorded slug parameter are then taken as demonstrated in Figure 1. Slug ascent velocity, i.e. the time taken for the nose (i.e. the part which remains most stable) of a single bubble to travel a marked distance of ~50 cm was determined using

$$v_b = d/t \qquad (8)$$

where v_b is ascent velocity, d is distance, and t is time. Bubble morphology was quantified where visibility was sufficient for measurement to observe any variability that occurs as a func-

tion of liquid and conduit properties. Measured parameters are combined with liquid and tube properties to derive the appropriate dimensionless parameters (Equations 1–3). Viscosity is determined mathematically using the mean Fr values for each mixture where $\theta = 0°$ by rearranging the Fr universal correlation (Equation 6) to calculate N_f:

$$N_f = \frac{31.08}{\left[\frac{1}{(2.94Fr)^{100/71}} - 1\right]^{20/29}} \qquad (9)$$

then μ was calculated by rearranging Equation 1 to give:

$$\mu = \frac{\rho\sqrt{gD^3}}{N_f}. \qquad (10)$$

Density was calculated using measured mixture mass and volume. Falling film thickness was not measured for this study due to insufficient visibility in media with PVF > 0. Video contrast is altered to resolve bubble visibility issues in particle-containing fluids (visibility for highest PVF values remained insufficient for accurate measurement). A more suitable crystal analogue or a better imaging technique is needed to constrain bubble behaviour in super-concentrated suspensions. The effect of lens distortion was quantified and expressed as an error value of 0.67 pixels, this is negligible given that the calculated mean reprojection error is <1 pixel [MathWorks 2021]. Typical variation in measured slug velocities through repeat experiments gave standard deviations of maximum ±0.0017.

4 Results and Discussion

Slug morphology, v_b, Fr, and Re are presented as functions of tube inclination angle (Table 3; Figures 4 and 5) and N_f (Figure 6). Each data point present on all plotted data represents the mean of ten experimental runs. For true scale volcanic comparison, the full range of dimensionless values observed throughout this study are: $0.17 \leq Fr \leq 0.52$, $3 \leq Re \leq 3300$, and $18 \leq N_f \leq 6354$; the full range for slug ascent velocity is $0.1 \leq v_b \leq 0.32$. Slug ascent velocity and associated dimensionless attributes (Fr, Re) show a trend of increase to a peak within the range $40° \leq \theta \leq 60°$, immediately followed by a decrease as a function of increasing inclination. Maxima occur in the lowest viscosity fluids within this inclination range and minima occur in the highest viscosity fluids, usually when $\theta = 0°$. The angles at which maximum proportional velocity change (Figure 5) occur (with respect to vertical tubes) are lower in low N_f media than in high N_f media and this shift to an earlier inclination is especially pronounced in the most viscous, highest PVF media. Bubble morphology also changes with inclination (Figure 7, Table 3), but no major deformation was observed as in Capponi et al. [2016] or Oppenheimer et al. [2020] because maximum PVF within this study is below the maximum packing fraction and bubble stability [identified by a closed, non-turbulent wake; Campos and Guedes De Carvalho 1988] is maintained for the full parameter range.

v_b is found to be a function of liquid properties (N_f, PVF) and tube inclination for the full range of measurements, and thus magmatic rheology (N_f, CVF) and internal conduit structure at true volcanic scale. Fr and Re behave similarly: their
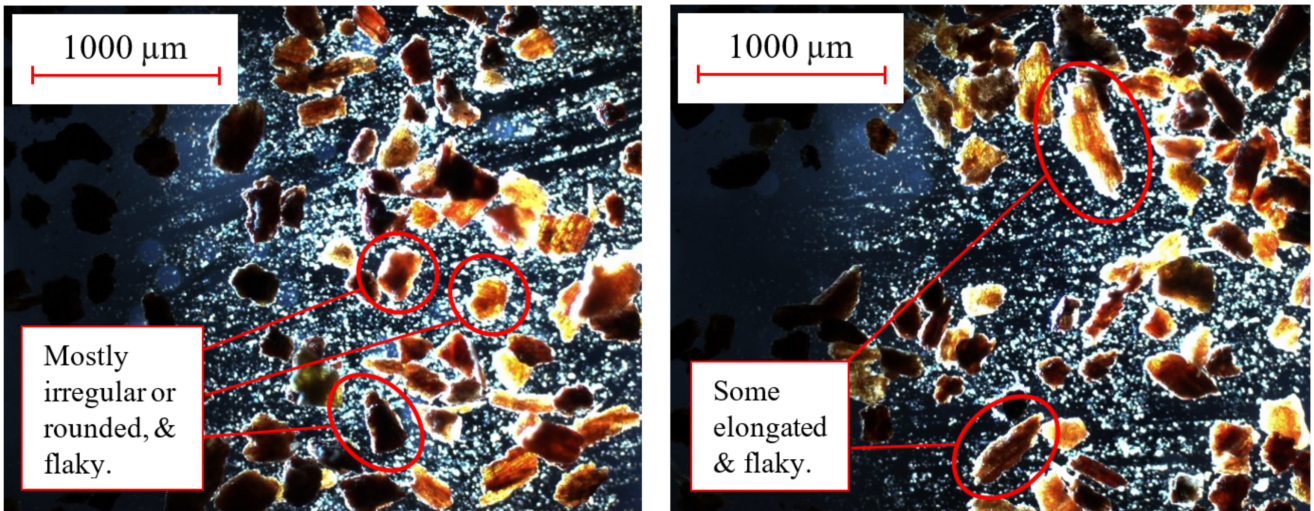
---

*https://imagej.nih.gov/ij/

Figure 3: Microscope images to display representative particle characteristics, taken using a Zeiss Axioplan 2 microscope at 40 times magnification. [A] Most particles have an irregular or rounded shape and [B] some are elongated; all appear flaky.
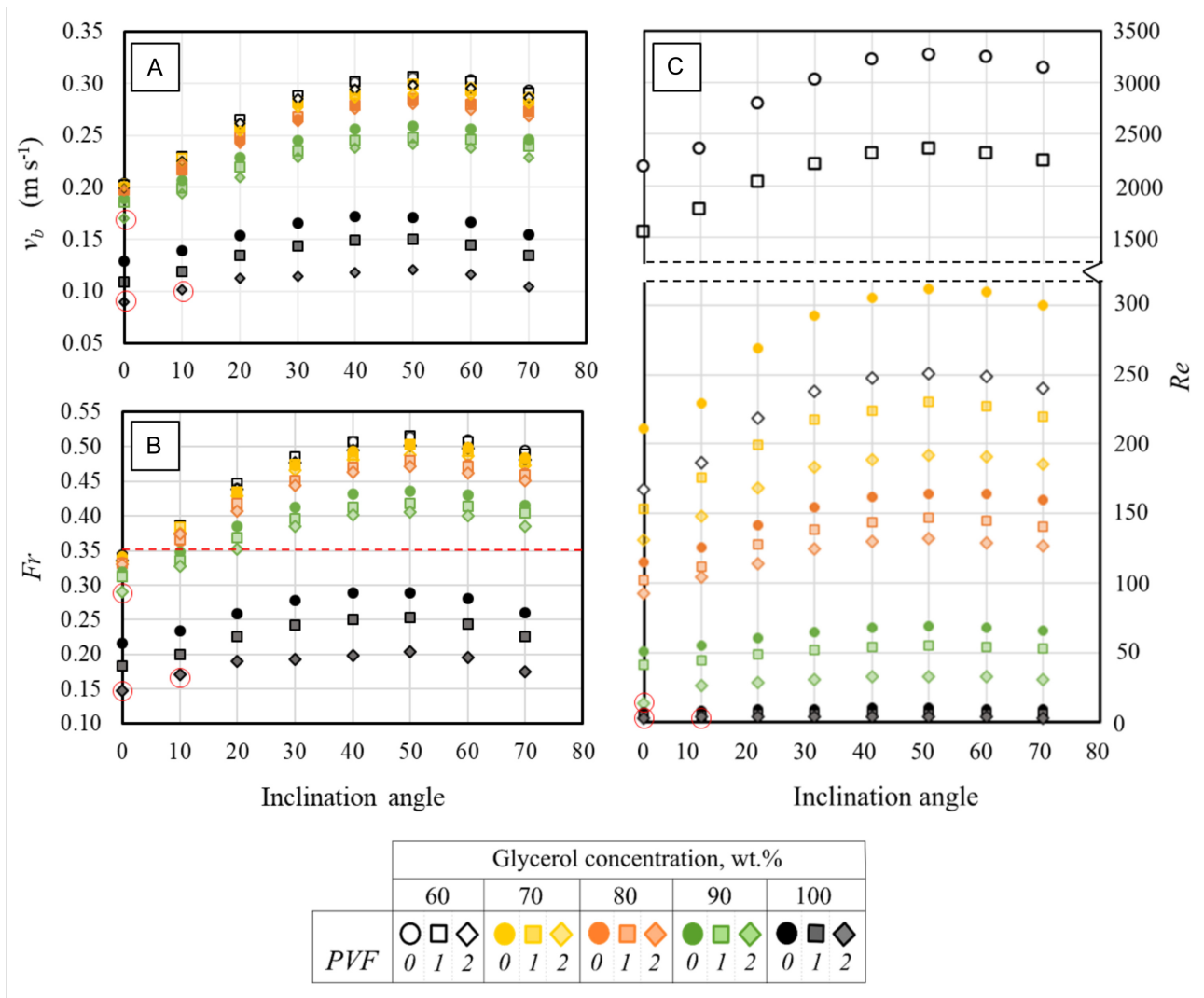

Figure 4: [A] Slug ascent velocity, [B] Froude number, and [C] Reynolds number as a function of tube inclination for the full range of N_f. The datapoints circled in red indicate extrapolated values where poor visibility inhibited direct measurement. The Fr constant is indicated by a dashed red line on plot [B]. Note that plot [C] has a split y axis.
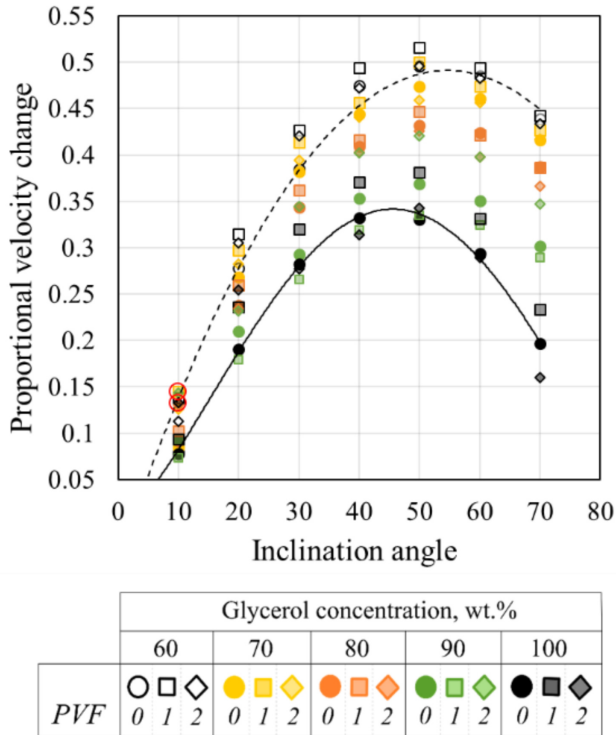
Figure 5: Change in slug ascent velocity, relative to $\theta = 0°$ (vertical), as a function of tube inclination angle for all liquid media. Note that PVF 2 data for 0° and 0°–10° in 90 wt.% and 100 wt.% solutions (circled in red) are based on the extrapolated velocity values seen in Figure 4A. The dashed and solid black lines indicate best fit (3rd order polynomial) for PVF 0, 60 wt.% glycerol and PVF 0, 100 wt.% solutions; note that the maxima occurs earlier in the lowest N_f media.

dependence on tube inclination angle decreases as viscous effects become more important, i.e. in lower N_f, or higher PVF media. Therefore, in vertical tubes they are a function of N_f only, but also become a function of inclination angle when $\theta > 0°$ because they are a function of v_b (Equations 2 and 3). The linear relationships of Re with N_f for the full range of inclination (Figure 6) demonstrates that Re has a strong dependence on N_f and also, to a lesser extent, inclination, i.e. for volcanic scenarios it is a function of N_f—which is a function of CVF and individual crystal properties—and conduit inclination when $\theta > 0°$. The full N_f range ($18 \leq N_f \leq 6354$) falls within the validity range proposed by Llewellin et al. [2012]. The effect of tube inclination angle on slug ascent velocity and associated parameters (Fr, Re) is complex and non-linear as a result of an observable change in bubble morphology that occurs in response to changing inclination and PVF. Qualitative changes in slug shape (Figure 7) have been observed to occur in response to increasing PVF in lower N_f media with increasing inclination. Bubble geometry remains axisymmetric where $\theta = 0°$ (vertical) as slugs rise through the centre of the tube, consistent with existing literature for both laboratory and volcanic scales [Davies and Taylor 1950; Campos and Guedes De Carvalho 1988; Viana et al. 2003; Llewellin et al. 2012; Capponi et al. 2016; Woitischek et al. 2020].

Slug ascent velocity is a function of nose shape [Pokusaev et al. 2011] or more specifically, the vicinity of nose curvature to its most critical point [de Azevedo et al. 2012] if it is independent of slug length, i.e. for $L_b > 1.5D$ [Shosho and Ryan 2001; James et al. 2004] and generally becomes blunter in lower N_f (i.e. high PVF and viscosity) fluids (Figure 7). Tail morphology becomes slightly rounded in vertical tubes when N_f is low ($79 \leq N_f \leq 122$) and bubbles shorten to a greater extent within this range, while slug diameter exhibits a slight increase (Table 3). These observations are accompanied by an overall decrease in slug ascent velocity for this inclination ($\theta = 0°$). As inclination increases slugs diverge from the central axis of the tube and adapt an asymmetric configuration (Figure 7) because the increasing influence of buoyancy forces the slugs up against the tube wall [Bendiksen 1984; James et al. 2004]) causing bubble morphology to deviate from the 'standard' slug structure (Figure 1). The relationships of D_b and L_b with inclination shift away from linear trends as PVF increases and the rate at which slugs elongate increases significantly within the range $40° \leq \theta \leq 70°$, especially in low N_f and high PVF media.

Slugs rising in particle-free media experience a change in nose shape from rounded to more oblate, while the tail is observed to flatten, elongate and thin with increasing tube inclination in agreement with previous literature [Figure 7; Zukoski 1966; James et al. 2006; Pokusaev et al. 2011; de Azevedo et al. 2015]. Slugs adopt a wedge-like shape as viscous effects become more important and the characteristic nose structure sharpens and flattens towards $\theta = 40°$, especially in the lowest N_f, particle-containing mixtures. However, only the tail maintains this structure for the full parameter range (up to $\theta = 70°$ and for $N_f \lesssim 34$) because nose curvature is observed to reduce and flatten to a point, away from its central axis (Figure 7). These observations are quantitatively supported by measurements of slug length L_b, and slug diameter D_b, which increase and decrease with increasing tube inclination, respectively (Table 3). Changes in slug structure influence ascent parameters because the increased contact between the slug and the tube wall due to increased buoyancy effects when $\theta > 0°$ triggers a modification of the overall drag coefficient and shape of the surrounding falling film [Bugg et al. 1998]. Maxima occur where the buoyancy forces driving bubble ascent are optimal ($40° \leq \theta \leq 60°$), and the subsequent decrease in v_b following this maximum can be attributed to these effects becoming resistive as inclination approaches a horizontal position, thus reducing overall velocity [Massoud et al. 2020].

When a system is in laminar flow, i.e. when the fluid is moving slowly and $Re < 2300$, as is the case here (with the exception of 60 wt.% PVF 0 and PVF 1 media; Figure 4), the contribution of viscous drag is increased and slug ascent velocity decreases. Particles are found to have a stabilizing effect on slug flow as a result of their overall effect of increasing viscosity, although there is uncertainty in the application of this statement to volcanic contexts where turbulence is driven by other factors (e.g. magmatic convection) and not magmatic viscosity alone. This shift in the maxima occurs with greater clarity in media with particularly low N_f and high PVF (Figure 4). The effect on proportional change in v_b (Figure 5)
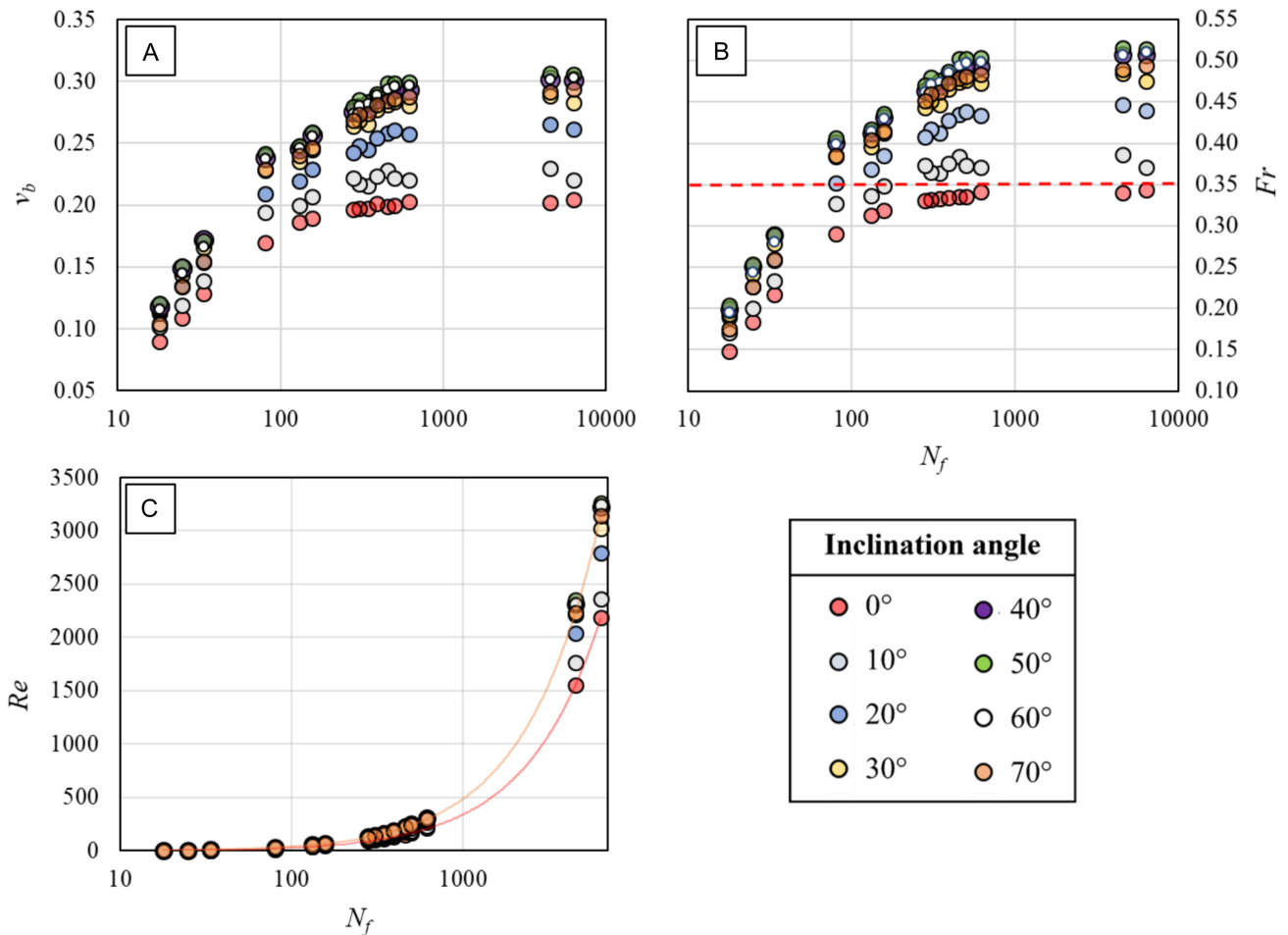
Figure 6: [A] Slug ascent velocity, [B] Froude number, and [C] Reynolds number as a function of N_f for the full range of inclination in all media. The Fr constant is indicated by a dashed red line on plot [B], and the linear relations for $\theta = 0°$ and $\theta = 70°$ only are given on plot [C].

is smaller as flow regimes become less stable, i.e. within higher N_f media and at lower inclinations, because the dependence of v_b on inclination decreases as viscous effects increase [Zukoski 1966; Massoud et al. 2020]. Higher PVF mixtures exhibit a rapid increase in viscosity, comparable to observations made in Mueller et al. [2011], Moitra and Gonnermann [2015], and Barth et al. [2019], and when added to low N_f solutions (>90 wt.% glycerol), according to our own observations. The overall trend in v_b because of these effects is a decreasing one, but the implications of this result on true-scale explosivity are complicated.

The level of explosivity achieved by individual eruptions is variable and highly complex: faster ascent and self-sustained slug expansion accelerates the overlying magma to accommodate for sudden gas volume change, increasing overpressure at burst and thus explosivity [Sonder et al. 2006; Oppenheimer et al. 2020]. However, high viscosity magmas are separately described to both enhance [Del Bello et al. 2012; Suckale et al. 2016] and reduce [Capponi et al. 2016] slug overpressure and thus, eruptive vigour. Generally, slugs rising in particle-bearing, higher viscosity suspensions accelerate slowly compared to in particle free media and the meniscus ruptures gen-

tly at burst, with no observable droplet ejection [Capponi et al. 2016; Rana et al. 2016] which translates to lower explosivity at volcanic scales.

The implications of our observations for the current estimations of volcanic-scale slug flow dynamics (specifically v_b) are best explained through Fr. Existing studies [Bugg et al. 1998; Seyfried and Freundt 2000; Shosho and Ryan 2001; James et al. 2004; Llewellin et al. 2012] observe that a constant of $Fr \approx 0.351$ is reached when viscous and surface tension forces are negligible (for $N_f > 300$ in vertical tubes/conduits and proportional to Re), consistent with potential flow theory. Similar behaviour has been inferred for volcanic scenarios, such as for Masaya in Nicaragua, which has a high N_f range ($518 \leq N_f \leq 4141$) relative to other basaltic volcanoes. There, Fr (0.345) remains constant for $D = 1.5$–6 m despite being a function of diameter (Equation 3). For volcanoes with relatively higher magmatic viscosity ($N_f < 300$) such as Yasur ($D = 1.5$–3 m), Erebus ($D = 3$–6 m), Stromboli ($D = \sim3$ m), and Etna ($D = 3$ m), Fr is observed to increase with increasing diameter (where conduits are assumed to be vertical). Our data is also in agreement with this where $\theta = 0°$: the total range of N_f covered is $18 \leq N_f \leq 6354$ and datapoints at this

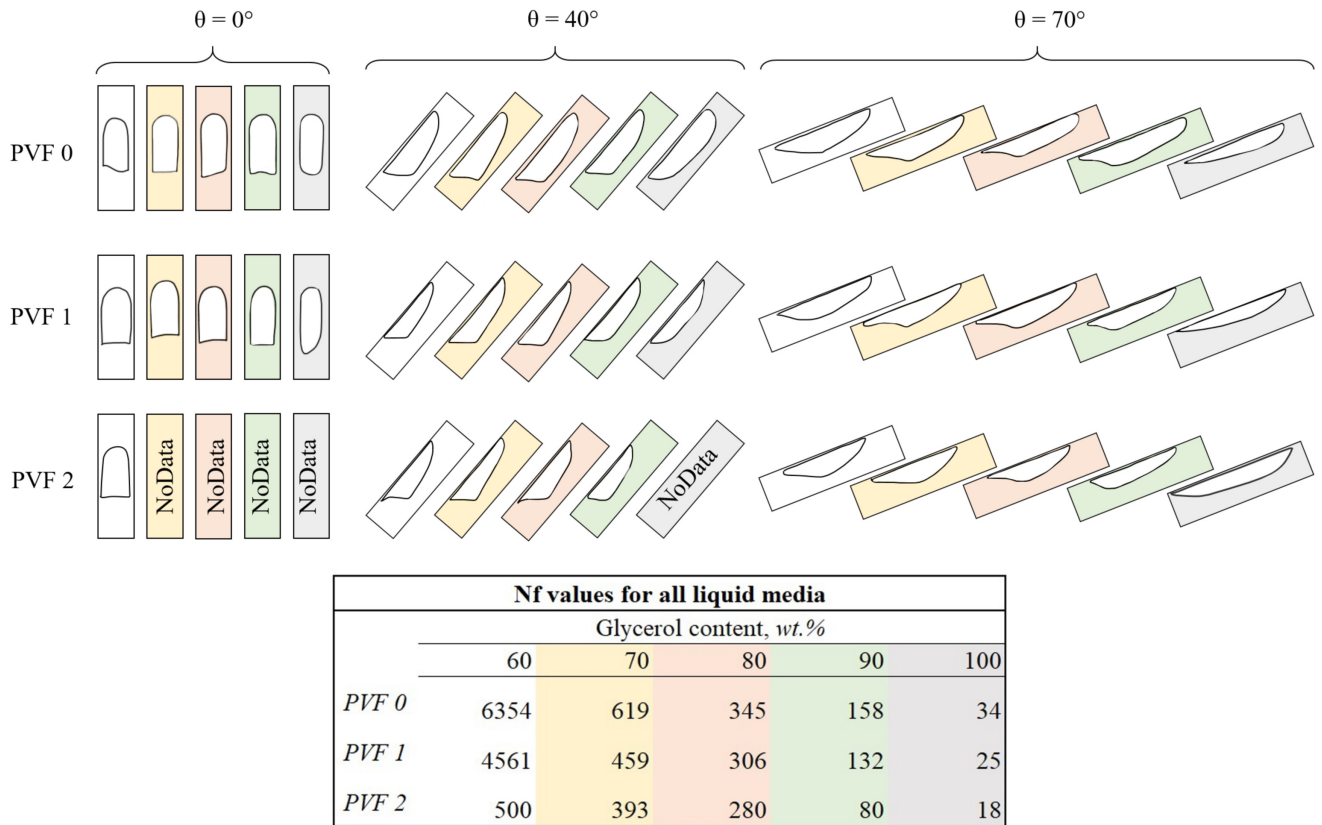Figure 7: Shape traces of representative bubble morphologies at three selected inclinations; θ = 0°, 40°, and 70°. 'NoData' indicates experiment runs where visibility was insufficient for measurement.

inclination where $N_f > 300$ are shown to remain constant at $Fr \approx 0.35$ (Figures 4B and 6B) . However, the Fr constant is surpassed in all cases where $\theta > 0°$ and $N_f > 300$ (Figure 6B), demonstrating that its use in current ascent velocity estimations for true-scale behaviour cannot be applied to natural, i.e. non-vertical, conduit systems.

The Fr constant is based on the assumption that the external flows surrounding bodies (i.e. the falling film around gas slugs in this context) are inviscid (frictionless) and irrotational [Bugg and Saad 2002]. This assumption becomes irrelevant when viscous effects become important [Llewellin et al. 2012] or when particles are added to a fluid (i.e. in magmas with high viscosity and CVF) because they change the bulk properties of the fluid, thus violating the assumption of potential flow. This also means the constant cannot be applied to this data set. The additional assumption of inertial control—indicated by laminar flow and a hemispherical nose [Bugg and Saad 2002] —by which the potential flow theory is also upheld is ambiguous in its relation to variable conduit inclination in volcanic environments because of the impact on slug morphology observed in experimental contexts when $\theta > 0°$, especially with increasing PVF (Figure 7).

5   CONCLUSIONS

Slug ascent velocity is illustrated as a function of tube inclination angle and liquid viscosity, which is in turn highly de-

pendent on particle characteristics. Dimensionless parameters (Fr, Re) were derived to describe specific flow characteristics and for the comparison of data from laboratory and volcanic scale scenarios. Slug morphology is highlighted as a strong function of PVF and inclination angle. Nose shape, specifically, is shown to be a strong function of v_b, especially within the inclination range of $40° \leq \theta \leq 60°$ and its relation to eruption explosivity as a function of slug overpressure is discussed qualitatively. CVF has a larger effect on slug ascent velocity in more viscous magmas within true-scale volcanic contexts. The internal geometries of shallow volcanic plumbing systems and the non-rheologically uniform nature of magma control for eruption explosivity as a direct consequence of their influence on gas ascent dynamics independently of (and in addition to) the controlling factors currently attributed to eruption modelling in the literature, i.e. magma viscosity, gas flux and related controlling characteristics. As an extension of Calleja and Pering [2021] this study predicts a shift in a higher parameter range, i.e. for v_b, Fr, and Re compared to values presented by existing literature due to the assumption of a uniform vertical conduit, which is rare in real volcanic scenarios. We have identified a clear and present need for the expansion of existing theoretical framework to accommodate for conduit inclination and rheologically stratified magma to accurately describe flow characteristics, perhaps through the development of a new dimensionless parameter, of which θ is a primary function.

Copyright notice

References

Armienti, P., L. Francalanci, and P. Landi (2007). "Textural effects of steady state behaviour of the Stromboli feeding system". *Journal of Volcanology and Geothermal Research* 160(1-2), pages 86–98. DOI: 10.1016/j.jvolgeores.2006.05.004.

Barth, A., M. Edmonds, and A. Woods (2019). "Valve-like dynamics of gas flow through a packed crystal mush and cyclic strombolian explosions". *Scientific Reports* 9(1). DOI: 10.1038/s41598-018-37013-8.

Bendiksen, K. H. (1984). "An experimental investigation of the motion of long bubbles in inclined tubes". *International Journal of Multiphase Flow* 10(4), pages 467–483. DOI: 10.1016/0301-9322(84)90057-0.

Bugg, J. D., K. Mack, and K. S. Rezkallah (1998). "A numerical model of Taylor bubbles rising through stagnant liquids in vertical tubes". *International Journal of Multiphase Flow* 24(2), pages 271–281. DOI: 10.1016/s0301-9322(97)00047-5.

Bugg, J. D. and G. A. Saad (2002). "The velocity field around a Taylor bubble rising in a stagnant viscous fluid: numerical and experimental results". *International Journal of Multiphase Flow* 28(5), pages 791–803. DOI: 10.1016/s0301-9322(02)00002-2.

Calleja, H. and T. Pering (2021). "Quantifying the influence of conduit inclination on Taylor Bubble behaviour in basaltic magmas." *EarthArXiv*. DOI: 10.31223/x5d04n. [Preprint].

Campos, J. B. L. M. and J. R. F. Guedes De Carvalho (1988). "An experimental study of the wake of gas slugs rising in liquids". *Journal of Fluid Mechanics* 196, pages 27–37. DOI: 10.1017/s0022112088002599.

Capponi, A., M. R. James, and S. J. Lane (2016). "Gas slug ascent in a stratified magma: Implications of flow organisation and instability for Strombolian eruption dynamics". *Earth and Planetary Science Letters* 435, pages 159–170. DOI: 10.1016/j.epsl.2015.12.028.

Capponi, A., S. J. Lane, and M. R. James (2017). "The implications of gas slug ascent in a stratified magma for acoustic and ground deformation source mechanisms in Strombolian eruptions". *Earth and Planetary Science Letters* 468, pages 101–111. DOI: 10.1016/j.epsl.2017.04.008.

Caricchi, L., L. Burlini, P. Ulmer, T. Gerya, M. Vassalli, and P. Papale (2007). "Non-Newtonian rheology of crystal-bearing magmas and implications for magma ascent dynamics". *Earth and Planetary Science Letters* 264(3-4), pages 402–419. DOI: 10.1016/j.epsl.2007.09.032.

Chouet, B., P. Dawson, T. Ohminato, M. Martini, G. Saccorotti, F. Giudicepietro, G. D. Luca, G. Milana, and R. Scarpa (2003). "Source mechanisms of explosions at Stromboli Volcano, Italy, determined from moment-tensor inversions of very-long-period data". *Journal of Geophysical Research: Solid Earth* 108(B1), ESE 7–1–ESE 7–25. DOI: 10.1029/2002jb001919.

Davies, R. M. and G. I. Taylor (1950). "The mechanics of large bubbles rising through extended liquids and through liquids in tubes". *Proceedings of the Royal Society of London. Series A. Mathematical and Physical Sciences* 200(1062), pages 375–390. DOI: 10.1098/rspa.1950.0023.

De Azevedo, M. B., D. dos Santos, N. N. Araujo, P. A. M. Vinhas, J. L. H. Faccini, and J. Su (2015). "Measurement of Interfacial Parameters of Single Taylor Bubbles Rising in Closed Vertical and Slightly Inclined Tubes Using Ultrasonic and Visualization Techniques." *23rd ABCM International Congress of Mechanical Engineering*. ABCM, Brazilian Society of Mechanical Sciences and Engineering. DOI: 10.20906/cps/cob-2015-0479.

De Azevedo, M. B., P. A. M. Vinhas, J. L. H. Faccini, and J. Su (2012). "Characterization of Velocity and Shape of Rising Bubbles in a Stagnant Liquid Vertical Column by Ultrasonic and Visualization Techniques". *14th Brazilian Congress of Thermal Sciences and Engineering*. ABCM, Brazilian Society of Mechanical Sciences and Engineering.

Del Bello, E., S. J. Lane, M. R. James, E. W. Llewellin, J. Taddeucci, P. Scarlato, and A. Capponi (2015). "Viscous plugging can enhance and modulate explosivity of strombolian eruptions". *Earth and Planetary Science Letters* 423, pages 210–218. DOI: 10.1016/j.epsl.2015.04.034.

Del Bello, E., E. W. Llewellin, J. Taddeucci, P. Scarlato, and S. J. Lane (2012). "An analytical model for gas overpressure in slug-driven explosions: Insights into Strombolian volcanic eruptions". *Journal of Geophysical Research: Solid Earth* 117(B2), B02206. DOI: 10.1029/2011jb008747.

Edmonds, M., M. C. S. Humphreys, E. H. Hauri, R. A. Herd, G. Wadge, H. Rawson, R. Ledden, M. Plail, J. Barclay, A. Aiuppa, T. E. Christopher, G. Giudice, and R. Guida (2014). "Chapter 16 Pre-eruptive vapour and its role in controlling eruption style and longevity at Soufrière Hills Volcano". *Geological Society, London, Memoirs* 39(1), pages 291–315. DOI: 10.1144/m39.16.

Gaudin, D., J. Taddeucci, P. Scarlato, E. Bello, T. Ricci, T. Orr, B. Houghton, A. Harris, S. Rao, and A. Bucci (2017). "Integrating puffing and explosions in a general scheme for Strombolian-style activity". *Journal of Geophysical Research: Solid Earth* 122(3), pages 1860–1875. DOI: 10.1002/2016jb013707.

Giordano, D., M. Polacci, P. Papale, and L. Caricchi (2010). "Rheological control on the dynamics of explosive activity in the 2000 summit eruption of Mt. Etna". *Solid Earth* 1(1), pages 61–69. DOI: 10.5194/se-1-61-2010.

Houghton, B., J. Taddeucci, D. Andronico, H. Gonnermann, M. Pistolesi, M. Patrick, T. Orr, D. Swanson, M. Edmonds, D. Gaudin, R. Carey, and P. Scarlato (2016). "Stronger or longer: Discriminating between Hawaiian and Strombolian eruption styles". *Geology* 44(2), pages 163–166. DOI: 10.1130/g37423.1.

James, M. R., S. J. Lane, and B. A. Chouet (2006). "Gas slug ascent through changes in conduit diameter: Laboratory insights into a volcano-seismic source process in low-viscosity magmas". *Journal of Geophysical Research: Solid Earth* 111(B5), B05201. DOI: 10.1029/2005jb003718.

James, M. R., S. J. Lane, B. A. Chouet, and J. S. Gilbert (2004). "Pressure changes associated with the ascent and bursting of gas slugs in liquid-filled vertical and inclined conduits". *Journal of Volcanology and Geothermal Research* 129(1-3), pages 61–82. DOI: 10.1016/s0377-0273(03)00232-4.

James, M. R., S. J. Lane, and S. B. Corder (2008). "Modelling the rapid near-surface expansion of gas slugs in low-viscosity magmas". *Geological Society, London, Special Publications* 307(1), pages 147–167. DOI: 10.1144/sp307.9.

James, M. R., S. J. Lane, L. Wilson, and S. B. Corder (2009). "Degassing at low magma-viscosity volcanoes: Quantifying the transition between passive bubble-burst and Strombolian eruption". *Journal of Volcanology and Geothermal Research* 180(2-4), pages 81–88. DOI: 10.1016/j.jvolgeores.2008.09.002.

Jaupart, C. and S. Vergniolle (1989). "The generation and collapse of a foam layer at the roof of a basaltic magma chamber". *Journal of Fluid Mechanics* 203, pages 347–380. DOI: 10.1017/s0022112089001497.

Jones, T. J., Y. L. Moigne, J. K. Russell, G. Williams-Jones, D. Giordano, and D. B. Dingwell (2022). "Inflated pyroclasts in proximal fallout deposits reveal abrupt transitions in eruption behaviour". *Nature Communications* 13(1). DOI: 10.1038/s41467-022-30501-6.

Kawaguchi, R. and T. Nishimura (2015). "Numerical investigation of temporal changes in volcanic deformation caused by a gas slug ascent in the conduit". *Journal of Volcanology and Geothermal Research* 302, pages 1–10. DOI: 10.1016/j.jvolgeores.2015.06.002.

Kawaji, M., J. M. DeJesus, and G. Tudose (1997). "Investigation of flow structures in vertical slug flow". *Nuclear Engineering and Design* 175(1-2), pages 37–48. DOI: 10.1016/s0029-5493(97)00160-x.

Knox, H. A., J. A. Chaput, R. C. Aster, and P. R. Kyle (2018). "Multiyear Shallow Conduit Changes Observed With Lava Lake Eruption Seismograms at Erebus Volcano, Antarctica". *Journal of Geophysical Research: Solid Earth* 123(4), pages 3178–3196. DOI: 10.1002/2017jb015045.

Llewellin, E. W., E. Del Bello, J. Taddeucci, P. Scarlato, and S. J. Lane (2012). "The thickness of the falling film of liquid around a Taylor bubble". *Proceedings of the Royal Society A: Mathematical, Physical and Engineering Sciences* 468(2140), pages 1041–1064. DOI: 10.1098/rspa.2011.0476.

Massoud, E. Z., Q. Xiao, and H. A. El-Gamal (2020). "Numerical study of an individual Taylor bubble drifting through stagnant liquid in an inclined pipe". *Ocean Engineering* 195, page 106648. DOI: 10.1016/j.oceaneng.2019.106648.

MathWorks (2021). *Single camera calibrator app*. URL: https://www.mathworks.com/help/vision/ug/using-the-single-camera-calibrator-app.html (visited on 03/01/2021).

Métrich, N., P. Allard, A. Aiuppa, P. Bani, A. Bertagnini, H. Shinohara, F. Parello, A. Di Muro, E. Garaebiti, O. Belhadj, and D. Massare (2011). "Magma and volatile supply to post-collapse volcanism and block resurgence in Siwi Caldera (Tanna Island, Vanuatu Arc)". *Journal of Petrology* 52(6), pages 1077–1105. DOI: 10.1093/petrology/egr019.

Mintz, B. G., B. F. Houghton, E. W. Llewellin, T. R. Orr, J. Taddeucci, R. J. Carey, U. Kueppers, D. Gaudin, M. R. Patrick, M. Burton, P. Scarlato, and A. L. Spina (2021). *Patterns of bubble bursting and weak explosive activity in an active lava lake—Halemaʻumaʻu, Kīlauea, 2015.* DOI: 10.3133/pp1867e. [Professional Paper 1867-E].

Moitra, P. and H. M. Gonnermann (2015). "Effects of crystal shape- and size-modality on magma rheology". *Geochemistry, Geophysics, Geosystems* 16(1), pages 1–26. DOI: 10.1002/2014gc005554.

Morgado, A. O., J. M. Miranda, J. D. P. Araújo, and J. B. L. M. Campos (2016). "Review on vertical gas–liquid slug flow". *International Journal of Multiphase Flow* 85, pages 348–368. DOI: 10.1016/j.ijmultiphaseflow.2016.07.002.

Mueller, S., E. W. Llewellin, and H. M. Mader (2011). "The effect of particle shape on suspension viscosity and implications for magmatic flows". *Geophysical Research Letters* 38(13), page L13316. DOI: 10.1029/2011gl047167.

Nigam, K. D. P., A. B. Pandit, and K. Niranjan (1995). "Effect of angle of inclination on liquid-phase controlled mass transfer from a gas slug". *Chemical Engineering Science* 50(2), pages 289–298. DOI: 10.1016/0009-2509(94)00234-i.

Oppenheimer, J., A. Capponi, K. V. Cashman, S. J. Lane, A. C. Rust, and M. R. James (2020). "Analogue experiments on the rise of large bubbles through a solids-rich suspension: A "weak plug" model for Strombolian eruptions". *Earth and Planetary Science Letters* 531, page 115931. DOI: 10.1016/j.epsl.2019.115931.

Oppenheimer, J., A. C. Rust, K. V. Cashman, and B. Sandnes (2015). "Gas migration regimes and outgassing in particle-rich suspensions". *Frontiers in Physics* 3. DOI: 10.3389/fphy.2015.00060.

Parfitt, E. A. (2004). "A discussion of the mechanisms of explosive basaltic eruptions". *Journal of Volcanology and Geothermal Research* 134(1-2), pages 77–107. DOI: 10.1016/j.jvolgeores.2004.01.002.

Pering, T. D., T. Ilanko, T. C. Wilkes, R. A. England, S. R. Silcock, L. R. Stanger, J. R. Willmott, R. G. Bryant, and A. J. S. McGonigle (2019). "A rapidly convecting lava lake at Masaya Volcano, Nicaragua". *Frontiers in Earth Science* 6. DOI: 10.3389/feart.2018.00241.

Pering, T. D. and A. J. S. McGonigle (2018). "Combining spherical-cap and Taylor bubble fluid dynamics with plume measurements to characterize basaltic degassing". *Geosciences* 8(2), page 42. DOI: 10.3390/geosciences8020042.

Pering, T. D., A. J. S. McGonigle, M. R. James, A. Capponi, S. J. Lane, G. Tamburello, and A. Aiuppa (2017). "The dynamics of slug trains in volcanic conduits: Evidence for expansion driven slug coalescence". *Journal of Volcanology and Geothermal Research* 348, pages 26–35. DOI: 10.1016/j.jvolgeores.2017.10.009.

Pering, T. D., A. J. S. McGonigle, M. R. James, G. Tamburello, A. Aiuppa, D. D. Donne, and M. Ripepe (2016). "Conduit dynamics and post explosion degassing on Stromboli: A combined UV camera and numerical modeling treatment". *Geophysical Research Letters* 43(10), pages 5009–5016. DOI: 10.1002/2016gl069001.

Pinto, A. M. F. R., M. N. C. Pinheiro, and J. B. L. M. Campos (1998). "Coalescence of two gas slugs rising in a co-current flowing liquid in vertical tubes". *Chemical Engineering Science* 53(16), pages 2973–2983. DOI: 10.1016/s0009-2509(98)00121-3.

Pokusaev, B. G., D. A. Kazenin, S. P. Karlov, and V. S. Ermolaev (2011). "Motion of a gas slug in inclined tubes". *Theoretical Foundations of Chemical Engineering* 45(5), pages 640–645. DOI: 10.1134/s0040579511050319.

Rana, B. K., A. K. Das, and P. K. Das (2016). "Asymmetric bursting of Taylor bubble in inclined tubes". *Physics of Fluids* 28(8), page 082106. DOI: 10.1063/1.4961040.

Seyfried, R. and A. Freundt (2000). "Experiments on conduit flow and eruption behavior of basaltic volcanic eruptions". *Journal of Geophysical Research: Solid Earth* 105(B10), pages 23727–23740. DOI: 10.1029/2000jb900096.

Shosho, C. E. and M. E. Ryan (2001). "An experimental study of the motion of long bubbles in inclined tubes". *Chemical Engineering Science* 56(6), pages 2191–2204. DOI: 10.1016/s0009-2509(00)00504-2.

Silva, M. C. F., J. B. L. M. Campos, and J. D. P. Araújo (2023). "3D numerical study of a single Taylor bubble rising along an inclined tube through Newtonian and non-Newtonian liquids". *Chemical Engineering and Processing – Process Intensification* 183, page 109219. DOI: 10.1016/j.cep.2022.109219.

Sonder, I., B. Zimanowski, and R. Büttner (2006). "Non-Newtonian viscosity of basaltic magma". *Geophysical Research Letters* 33(2). DOI: 10.1029/2005gl024240.

Sparks, R. S. J. (2003). "Dynamics of magma degassing". *Geological Society, London, Special Publications* 213(1), pages 5–22. DOI: 10.1144/gsl.sp.2003.213.01.02.

– (1978). "The dynamics of bubble formation and growth in magmas: A review and analysis". *Journal of Volcanology and Geothermal Research* 3(1-2), pages 1–37. DOI: 10.1016/0377-0273(78)90002-1.

Spina, L., A. Cannata, D. Morgavi, and D. Perugini (2019). "Degassing behaviour at basaltic volcanoes: New insights from experimental investigations of different conduit geometry and magma viscosity". *Earth-Science Reviews* 192, pages 317–336. DOI: 10.1016/j.earscirev.2019.03.010.

Suckale, J., J.-C. Nave, and B. H. Hager (2010a). "It takes three to tango: 1. Simulating buoyancy-driven flow in the presence of large viscosity contrasts". *Journal of Geophysical Research* 115(B7). DOI: 10.1029/2009jb006916.

Suckale, J., B. H. Hager, L. T. Elkins-Tanton, and J.-C. Nave (2010b). "It takes three to tango: 2. Bubble dynamics in basaltic volcanoes and ramifications for modeling normal Strombolian activity". *Journal of Geophysical Research* 115(B7). DOI: 10.1029/2009jb006917.

Suckale, J., T. Keller, K. V. Cashman, and P.-O. Persson (2016). "Flow-to-fracture transition in a volcanic mush plug may govern normal eruptions at Stromboli". *Geophysical Research Letters* 43(23). DOI: 10.1002/2016gl071501.

Vergniolle, S. and C. Jaupart (1990). "Dynamics of degassing at Kilauea Volcano, Hawaii". *Journal of Geophysical Research* 95(B3), page 2793. DOI: 10.1029/jb095ib03p02793.

Viana, F., R. Pardo, R. Yánez, J. L. Trallero, and D. D. Joseph (2003). "Universal correlation for the rise velocity of long gas bubbles in round pipes". *Journal of Fluid Mechanics* 494, pages 379–398. DOI: 10.1017/s0022112003006165.

Viccaro, M., A. Cannata, F. Cannavó, R. De Rosa, M. Giuffrida, E. Nicotra, M. Petrelli, and G. Sacco (2021). "Shallow conduit dynamics fuel the unexpected paroxysms of Stromboli volcano during the summer 2019". *Scientific Reports* 11(1). DOI: 10.1038/s41598-020-79558-7.

Vona, A., C. Romano, D. Dingwell, and D. Giordano (2011). "The rheology of crystal-bearing basaltic magmas from Stromboli and Etna". *Geochimica et Cosmochimica Acta* 75(11), pages 3214–3236. DOI: 10.1016/j.gca.2011.03.031.

Wallis, G. B. (1969). *One-dimensional two-phase flow.* McGraw-Hill, New York, page 408. ISBN: 9780070679429.

White, E. and R. Beardmore (1962). "The velocity of rise of single cylindrical air bubbles through liquids contained in vertical tubes". *Chemical Engineering Science* 17(5), pages 351–361. DOI: 10.1016/0009-2509(62)80036-0.

Woitischek, J., M. Edmonds, and A. W. Woods (2020). "The control of magma crystallinity on the fluctuations in gas composition at open vent basaltic volcanoes". *Scientific Reports* 10(1). DOI: 10.1038/s41598-020-71667-7.

World Health Organization (2002). *The world health report 2002: reducing risks, promoting healthy life.* World Health Organization. ISBN: 92-4-156207-2.

Yamamoto, M., H. Kawakatsu, S. Kaneshima, T. Mori, T. Tsutsui, Y. Sudo, and Y. Morita (1999). "Detection of a crack-like conduit beneath the active crater at Aso Volcano Japan". *Geophysical Research Letters* 26(24), pages 3677–3680. DOI: 10.1029/1999gl005395.

Zandomeneghi, D., R. Aster, P. Kyle, A. Barclay, J. Chaput, and H. Knox (2013). "Internal structure of Erebus volcano, Antarctica imaged by high-resolution active-source seismic tomography and coda interferometry". *Journal of Geophysical Research: Solid Earth* 118(3), pages 1067–1078. DOI: 10.1002/jgrb.50073.

Zukoski, E. E. (1966). "Influence of viscosity, surface tension, and inclination angle on motion of long bubbles in closed tubes". *Journal of Fluid Mechanics* 25(4), pages 821–837. DOI: 10.1017/s0022112066000442.